


Article

Abrasion Power of Ti and Ni Diamond-Coated Coatings Deposited by Cold Spray

Raffaella Sesana ^{1,*} , Rocco Lupoi ², Irene Pessolano Filos ¹, Pengfei Yu ² and Sebastiano Rizzo ³¹ DIMEAS, Politecnico di Torino, Corso Duca Degli Abruzzi 24, 10129 Torino, Italy; irene.pessolano@polito.it² Department of Mechanical, Manufacturing & Biomedical Engineering, Trinity College Dublin, The University of Dublin, Parsons Building, D02 PN40 Dublin, Ireland; lupoir@tcd.ie (R.L.); yup1@tcd.ie (P.Y.)³ Central Lab–Product Development, Tsubaki Nakashima, Corso Torino, 378, 10064 Pinerolo (TO), Italy; sebastiano.rizzo@europe.tsubaki-nakashima.com

* Correspondence: raffaella.sesana@polito.it; Tel.: +39-011-0906907

Abstract: In this work, the cold spray technique was used to deposit nickel and titanium coated diamond powder on cast iron and aluminum substrates. To analyze the deposition mechanism, the diamond powders were observed before and after the process using a microscope and scanning electron microscope (SEM). The adhesion response of the Ni and Ti coatings was investigated during the study. Pin-on-disk tests were then performed to identify the abrasion mechanism of the coated samples and the wear resistance of the Si₃N₄ ceramic balls. Experimental tests were adopted to determine the significant operating variables, i.e., the local linear speed and the applied load. The modification of the diamond particles in shape, distribution, and the residual debris of Si₃N₄ on disk were compared before and after the tribological test to analyze the abrasion and wear resistance of the ceramic balls.

Keywords: cold spray; coated diamond powder; wear test; ceramic balls production; abrasion power; tribology



Citation: Sesana, R.; Lupoi, R.; Pessolano Filos, I.; Yu, P.; Rizzo, S. Abrasion Power of Ti and Ni Diamond-Coated Coatings Deposited by Cold Spray. *Metals* **2022**, *12*, 1197. <https://doi.org/10.3390/met12071197>

Academic Editor: Hamid Jahed

Received: 16 May 2022

Accepted: 12 July 2022

Published: 14 July 2022

Publisher's Note: MDPI stays neutral with regard to jurisdictional claims in published maps and institutional affiliations.



Copyright: © 2022 by the authors. Licensee MDPI, Basel, Switzerland. This article is an open access article distributed under the terms and conditions of the Creative Commons Attribution (CC BY) license (<https://creativecommons.org/licenses/by/4.0/>).

1. Introduction

Hybrid bearings represent an interesting engineering solution for mechanical applications in the automotive and aerospace industries or when electrical and thermal isolation, mechanical wear resistance, durability, and reliability are required [1]. These components are designed with a consolidated geometry and well-known materials and still present challenging issues related to applications and manufacturing. Recently, dedicated investigations were developed with the aim of extending life models to these components, as different materials, i.e., ceramic for the rolling elements and metals for the races, are involved [2–4]. These damage models include the surface microgeometry aspects as factors affecting fatigue resistance and lubrication behavior in the computation of expected life. Microgeometry and density are related to the manufacturing process especially with regard to ceramic rolling bodies, as the rolling bodies are generally obtained by sintering and subsequent surface finish. This process is performed by a couple of cast iron fixed and rotating plates, where grooves are obtained. While the disk rotates, the balls in the grooves are processed by diamond paste. The manufacturing time for a batch of ceramic balls is roughly 10 times longer than for steel balls and is also polluting and expensive. A possible alternative process consists of preprocessing the ceramic balls by means of grooves coated by abrasive coatings to obtain the diameter, roundness, and geometrical requirements, leaving only the final lapping phase to the diamond paste processing, according to similar processes performed on metallic balls. According to this procedure, when processed in rotating grooves, the balls rotate and displace in different positions, thus being subjected to different abrasion speeds. The necessity of finding new abrasive coatings, with specific

requirements related both to ball abrasive performance and to abrasive coating adhesion to grooves, is growing stronger in the ceramic ball production industry.

The cold spray (CS) technique is a potential method for coating deposition due to the complex shape of the grooves on the disk. Metals, polymers, ceramics, composite materials, and nanocrystalline powders can be deposited using cold spraying. The kinetic energy of the particles, supplied by the expansion of the gas, is converted to plastic deformation energy during bonding. Unlike other thermal spraying techniques, e.g., plasma spraying, arc spraying, flame spraying, or high velocity Oxygen fuel (HVOF), in CS the powders are not melted during the spraying process [5], but a plastic deformation process occurs generating the adhesion of the particles to the substrate. Several factors affect the coating deposition in the coating process and in particular in the cold spray process. Ref. [6] investigates the relationship between the particle flow and its acceleration in the nozzle. All the input parameters play a fundamental role in the adhesion of the coating on the substrate. The deposition on the metallic surface requires low solubility of carbon, and the process is affected by substrate temperature, carbon concentration, and the carbon diffusion coefficient. The chemical reaction is also influential, in fact the iron can absorb the carbon postponing the coating adhesion. Moreover, iron and other metals have an elevated vapor pressure that can contaminate the diamond formation in the surrounding area [7]. Diamond-like carbon coating adhesion on 316L stainless steel has been investigated in [8]. Carburizing pre-treatment and superficial etching seem to increase the adhesion properties; moreover, a cleaning and deoxidation procedure of the surface has been considered. Few literature papers were found to the authors' knowledge, on the abrasion performance of coatings and in particular in cold sprayed coatings, quantifying the performance and the effectiveness of the procedure. Most of them are focused on the adhesion properties of the diamond particles to the coating [7,9], or to the adhesion of the coating to the substrate [8,10], or on the influence of the interlayer in the adhesion mechanisms [8,11]. The abrasion of ceramic components by means of diamond coating is investigated in [12], but the analysis is focused not on the abrasion process but on the effectiveness of the process on different ceramics, measured only by means of the *Ra* roughness parameter.

In this framework, the aim of the research is to evaluate the applicability of the cold spray technique for obtaining a performant abrasive coating to be used in ball ceramic processing.

The cold spray technique adapts well to this application due to the ability to orient the spray to coat complex geometries such as the grooves in the disks. Furthermore, in cold spray no oxidation of the powder takes place during the process, and the material properties are preserved [13].

The aim of this paper is to investigate the deposition mechanism on cast iron and on aluminum alloy of diamond particles by means of cold spray. To this aim, two batches of diamond particles, with different deposition parameters, were deposited on two substrates, cast iron, which is the commercial material of which the processing disks are made, and aluminum, to preliminarily investigate the possibility of obtaining lighter disks. A further aim of the paper is the analysis of the abrasive behavior of the diamond coating deposited on the ceramic balls. To this aim, pin-on-disk tests were performed for different abrasion speeds on a batch of 6 mm ceramic balls. Profile, roughness, and wear parameter measurements were then performed on the sample to quantify and qualify the process for different rotating speeds.

2. Materials and Methods

The problem of setting up a new manufacturing process involves different issues related to component design, materials, process parameters setup, and performance evaluation. In this paper, a preliminary investigation is performed on the abrasion of the ceramic balls by means of abrasive coatings.

The experimental investigation described in this paper involved the use of two different commercial diamond powders, with different coatings (Ni and Ti), and cast iron and aluminum alloy substrates.

Sample preparation was carried out as described in Section 2.1 in collaboration between the Politecnico di Torino (Torino, Italy), the Tsubaki Nakashima Internal Application Laboratory (Pinerolo, Torino, Italy), and the STAM Research Center of the Department of Mechanical, Manufacturing and Biomedical Engineering at Trinity College Dublin (Dublin, Ireland). In particular, the CS deposition system used is described in [5,6]. The tribological experimental campaign described in Section 2.2 was carried out in the Department of Mechanical and Aerospace Engineering Laboratory (DIMEAS) of the Politecnico di Torino (Italy) employing Si₃N₄ ceramic bearing balls (nominal diameter 6 mm).

2.1. Materials

Cast iron and the aluminum alloy were selected as substrates. The cast iron samples were obtained from a cast iron disk used in ceramic ball manufacturing lines. The aluminum alloy sample was preliminarily selected to examine the possibility of preparing lighter abrasive disks. The chemical composition of the substrates was analyzed using the scanning electron microscope and the weight of elements in % is reported in Table 1.

Table 1. Substrates chemical composition.

Cast Iron 1	C (%)	Si (%)	P (%)	Fe (%)	Ni (%)
	12.68	0.66	0.02	86.63	0.01
Cast Iron 2	C (%)	Si (%)	P (%)	Fe (%)	Ni (%)
	9.8	1.64	0.81	83.63	4.12
Al Alloy	C (%)	O (%)	Al (%)	P (%)	Ni (%)
	36.03	5.23	56.41	0.54	1.79

The diamond powders selected are the Ti-RVD titanium-coated powder (Ti-Dia) and the Ni-RVD nickel-coated powder (Ni-Dia). In this paper gives an overview of the behavior of the two different coatings in the abrasion of ceramic balls. The 304L and 316L stainless steel powders for interlayer preparation were provided by LPW Technology, while the titanium diamond powder was supplied by HNHONGXIANG (Zhengzhou, China) and the nickel diamond powder by Shilidiamond (Changsha, China).

The dimension D50 of the 304L and 316L interlayer powders was 28 μm (D10 19 μm and D90 42 μm) and 33 μm (D10 21 μm and D90 45 μm), respectively (Figure 1).

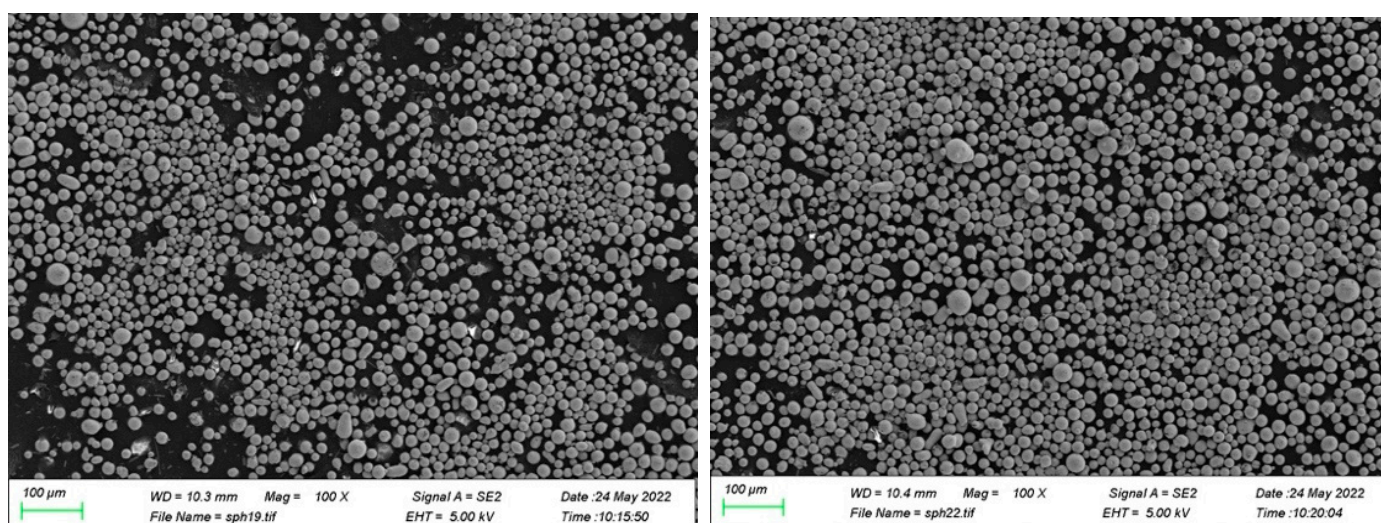


Figure 1. Interlayer powder particles, 304L (left) and 316L (right) (SEM).

Before the CS deposition, the two diamond powders were analyzed under a digital microscope (Figure 2). The diamond particles appeared sharp and edge. The powder samples dimensions were measured. The Ni-Dia powder's dimension D50 was 125.4 μm (D10 75.8 μm and D90 141.1 μm), while Ti-Dia was 111.1 μm (D10 84.0 μm and D90 125.9 μm). These large powder dimensions were selected according to the requirements of the abrasion production process of the ceramic balls for hybrid bearings.

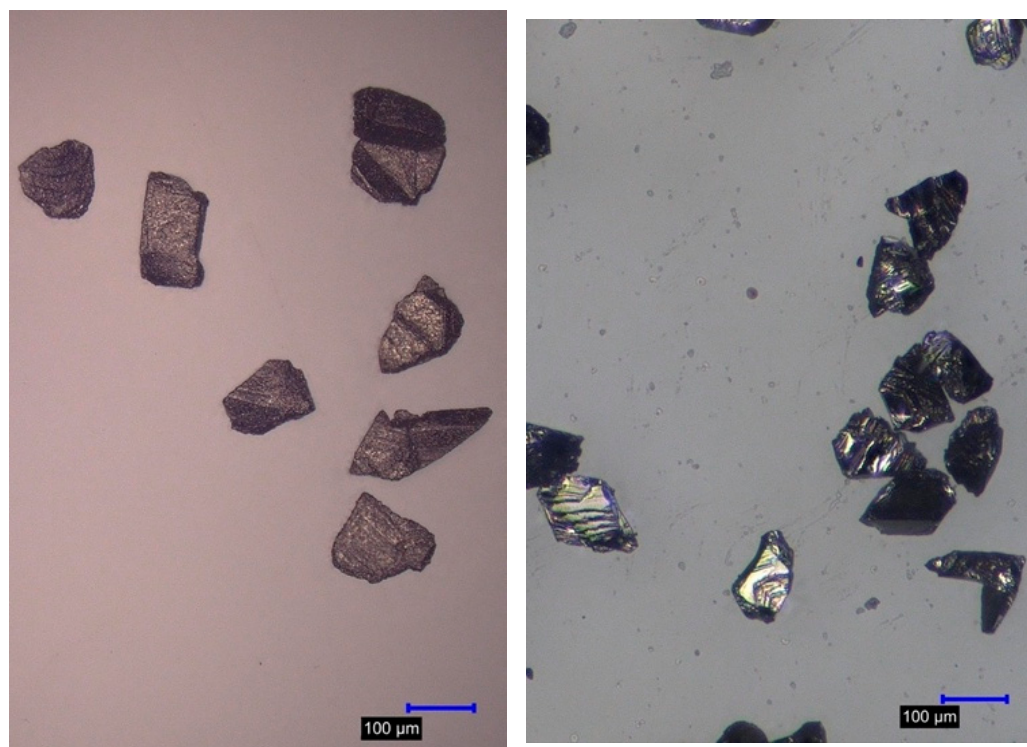


Figure 2. Diamond powders particles, Ni-Dia (left) and Ti-Dia (right) (optical microscope).

Furthermore, before coating the specimens by means of CS, customized flow tests of the diamond powders were run. The flow test is an indicator for material and flow powder disposition to cold spraying, as the correct flow through the nozzle is essential for a uniform coating deposition. In the test, the powder flow is tested through a funnel with a 50 mm diameter exit. The funnel during the test is steady. The powder should flow very rapidly and easily through the funnel. As a result of the flow test, the Ni-coated diamond particles had a better performance than Ti-coated diamond particles.

Several coated samples were prepared by varying the process parameters, keeping the hatch distance set to 4 mm. In Table 2 the sample preparation settings are reported.

Table 2. Coating specimen preparation: deposition parameters.

Test	Substrate	TS * (mm/s)	p (bar)	Carrier Gas	Gas T (°C)	PFR ** (%)	SoD *** (mm)	Powder
305	Cast iron	2400	30	N ₂	800	11	40	316L
307	Cast iron	2400	30	N ₂	850	11	40	304L
309	Cast iron	1200	30	N ₂	850	11	40	304 + Ti-Dia
310	Cast iron	1200	30	N ₂	850	11	40	304 + Ni-Dia
315	Aluminum	1200	30	N ₂	850	11	40	304 + Ni-Dia
314	Aluminum	1200	30	N ₂	850	11	40	304 + Ti-Dia

* Transverse Speed (TS) of the nozzle; ** PFR Power Feed Rate, percent of the maximum wheel rotation; *** SoD Distance between the nozzle and the substrate.

Before the coating process, the samples were ground with a P320 abrasive paper to improve the adhesion of the coating to the substrate [3]. The processing powders were

dried in the furnace at 200 °C for about 2 h before the experiments began. Following the procedure reported in [9,14–20], the cold spray deposition process was performed.

Tests 306 and 307 were dedicated to investigating the adhesion of a steel interlayer to cast iron. The test provided a useful sample: adhesion between 316L (interlayer) and cast iron (substrate) was efficient. In test 307 the layers adhered well to only one sample, while on two other samples the adhesion was moderate and in one sample the layer detached.

In Test 309 the Ti-Dia powder was cold sprayed on a sample without interlayer and on a sample with 304 steel interlayer and only the sample without interlayer was successful; the diamond coating adhesion on cast iron was effective. The mixture for abrasive coating deposition was 50% weight diamond powder and 50% weight 304 steel.

Test 310 replicated test 309 but with Ni-coated diamond powder instead of the Ti-coated one. The coating did not stick on the sample without interlayer.

Test 314 performed Ti diamond powder coating on an aluminum substrate, without interlayer. The experiment was successful, and the diamond coating adhered to the substrate.

Test 315 replicated test 314 but with Ni diamond powder coating. The sample was successful.

Two samples were then selected and used for the subsequent pin-on-disk testing, which is the aluminum one due to the better adhesion results. As the abrasion performance was the indicator for the test, the cast iron samples were excluded due to the non-optimized adhesion process. In Figure 3, some samples are reported: Figure 3 left, Test 310 sample shows inadequate adhesion of coating to the cast iron sample, while excellent sticking has been achieved with the aluminum substrates (Figure 3 center and right). In Figure 4, the SEM of coating surfaces is reported. Coating thickness was approximatively 1 mm.

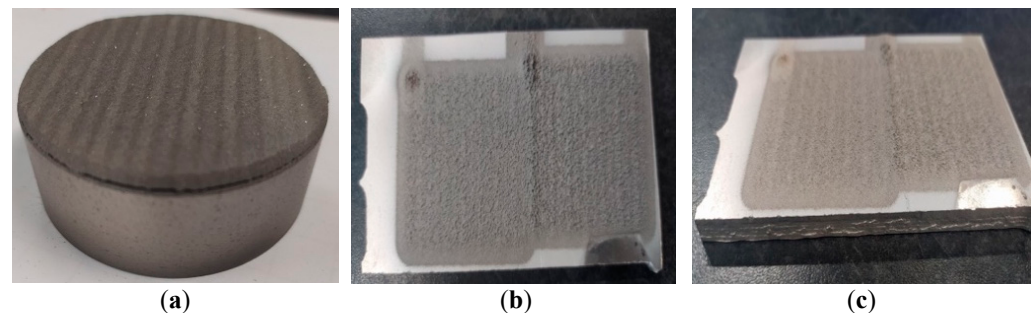


Figure 3. Cast Iron (a) and Al alloy (b,c) samples.

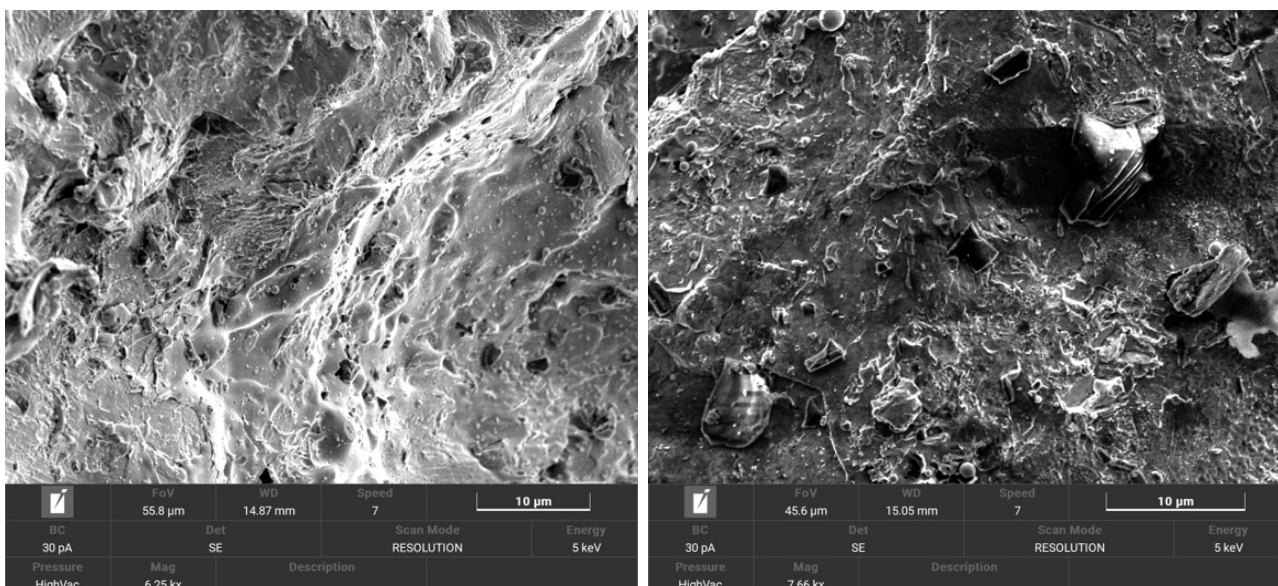


Figure 4. SEM images of coating surface: Ni-Dia (left) and Ti-Dia (right).

Before running the wear tests, the roughness measurements were performed on the pin (Si3N4 balls) (Table 3). Roughness was also measured for the disks considering three different measurement points (Figure 5). Measuring length was 5 mm and three measurements were run in each position. The measuring length and the cutoff (sampling length) were selected considering surface roughness values, according to ISO 4288 (Tables 1 and 2). It has to be noted that, for left and right measurements, the measuring direction is radial, while for the top measurement the measuring direction is perpendicular to the radius, which is along the wear race. The average roughness values measured on the disks in each position are reported in Table 4. It can be observed that the roughness is homogeneously distributed, thus indicating that the deposition process was not affected by inhomogeneity of particle distribution. A further observation can be made: before cold spraying, the Ti-coated diamond particles are generally smaller than the Ni-coated diamond particles. Conversely, after cold spraying, the Ni-coated specimen presents surface roughness values which are lower than the Ti-coated specimen. This difference may be partially due to the different behavior in flow through the nozzle of the two powders, where the Ni powders showed a better flow behavior than the Ti powders.

Table 3. Surface roughness of balls (pin) before wear tests (average values).

		R_a (μm)	R_q (μm)	R_p (μm)	R_v (μm)	R_z (μm)
Si3N4 ball	Before test	0.0067	0.0096	0.0189	0.0796	0.0922

Table 4. Surface roughness of coated disks before wear tests in three different points.

		R_a (μm)	R_q (μm)	R_p (μm)	R_v (μm)	R_z (μm)
Al alloy-Ti coated	Right	129	147	269	215	484
	Left	100	123	196	271	467
	Top	135	159	298	299	597
Average		121	143	254	261	516
Al alloy-Ni coated	Right	63	72	125	132	257
	Left	33	40	86	73	159
	Top	50	65	114	150	264
Average		48	59	108	118	226

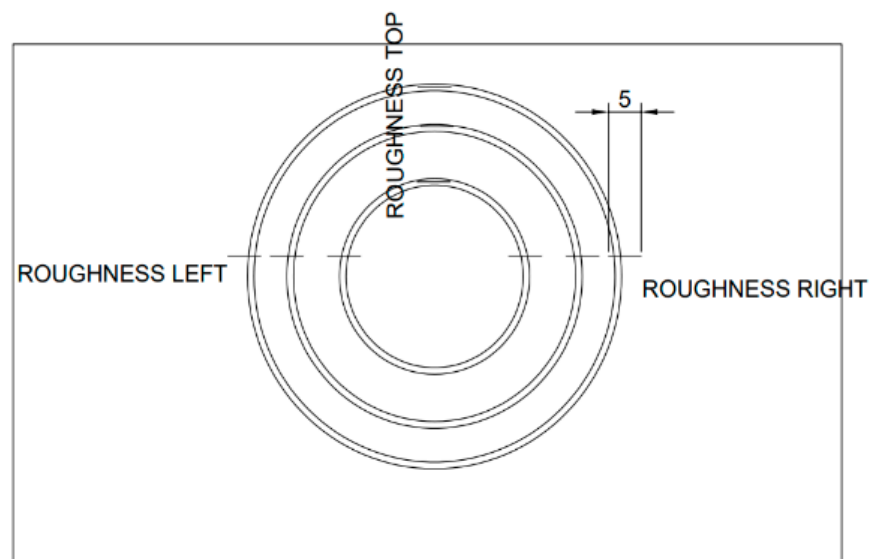


Figure 5. Disks points of roughness measurements (dimension in mm).

2.2. Test Methods

After the CS deposition, the aluminum alloy substrates were selected to carry out the pin-on-disk wear test in dry conditions. Tests were performed by means of an Anton Paar TRB tribometer compliant with the ASTM G99 and ASTM G133 standards [21,22]. Testing conditions adopted for the experimental campaign are reported in Table 5 according to previous studies and scientific literature [23–25]. In particular, local linear speed was varied, while the length run L was the same for all specimens (150 m). The normal preload F_N was the same for all tests, 5N, and the radius of contact between the pin and the rotation axis R_t was varied (7, 11, and 14 mm), while the rotational speed n was the same for all specimens at 20 rpm. A similar procedure was set up and then applied in [26], where a diamond-reinforced metal matrix composite was cold-sprayed on an aluminum substrate and a synthetic diamond coating with a maximum particle size of 30 μm was electrodeposited on a cast iron substrate.

Table 5. Testing parameters configuration for pin-on-disk tests.

Test Number	Coating Type	R_t (mm)	F_N (N)	n (rpm)	Local Linear Speed (mm/s)	L (m)
Test 1	Ni Dia	7	5	20	14.66	150
Test 2	Ni Dia	11	5	20	23.04	150
Test 3	Ni Dia	14	5	20	29.32	150
Test 4	Ti Dia	7	5	20	14.66	150
Test 5	Ti Dia	11	5	20	23.04	150
Test 6	Ti Dia	14	5	20	29.32	150

The experimental campaign was carried out and the data were processed according to Archard's equations and following the procedure reported in [26]. In particular, the roughness was measured on the abrasive disks, and on the abraded pins (the balls) the abraded volume of the ball (volume loss) V_b (mm^3) was measured. The wear rate u ($\mu\text{m}/\text{h}$) and the wear coefficient k were also obtained.

3. Results and Discussion

The different abrasive behavior of the two considered coatings (Ti and Ni diamond-coated powders) employed in the manufacturing processes of ceramic ball bearings were analyzed, and the results processed.

In the following Figure 6, the worn surfaces after pin-on-disk test are reported.

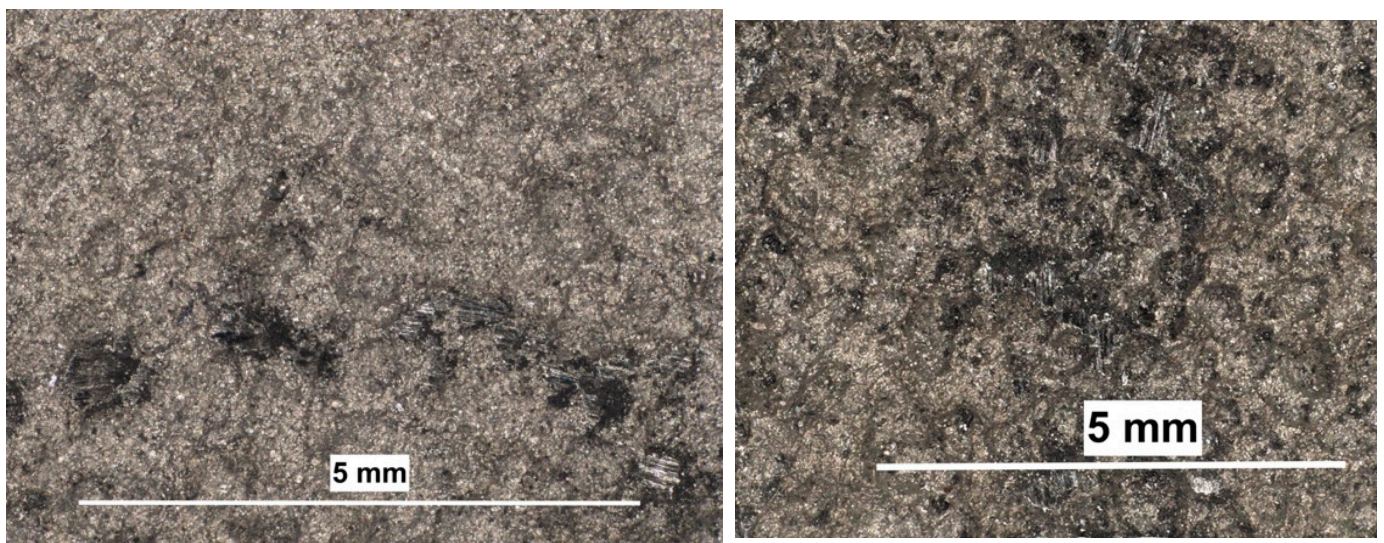


Figure 6. Worn surfaces after pin-on-disk tests, Ni-Dia (left) and Ti-Dia (right) (optical microscope).

The results obtained after pin-on-disk testing are graphically reported in Figure 7. In particular, the values of roughness are compared considering for both the balls and the substrates the values between after and before the wear tests.

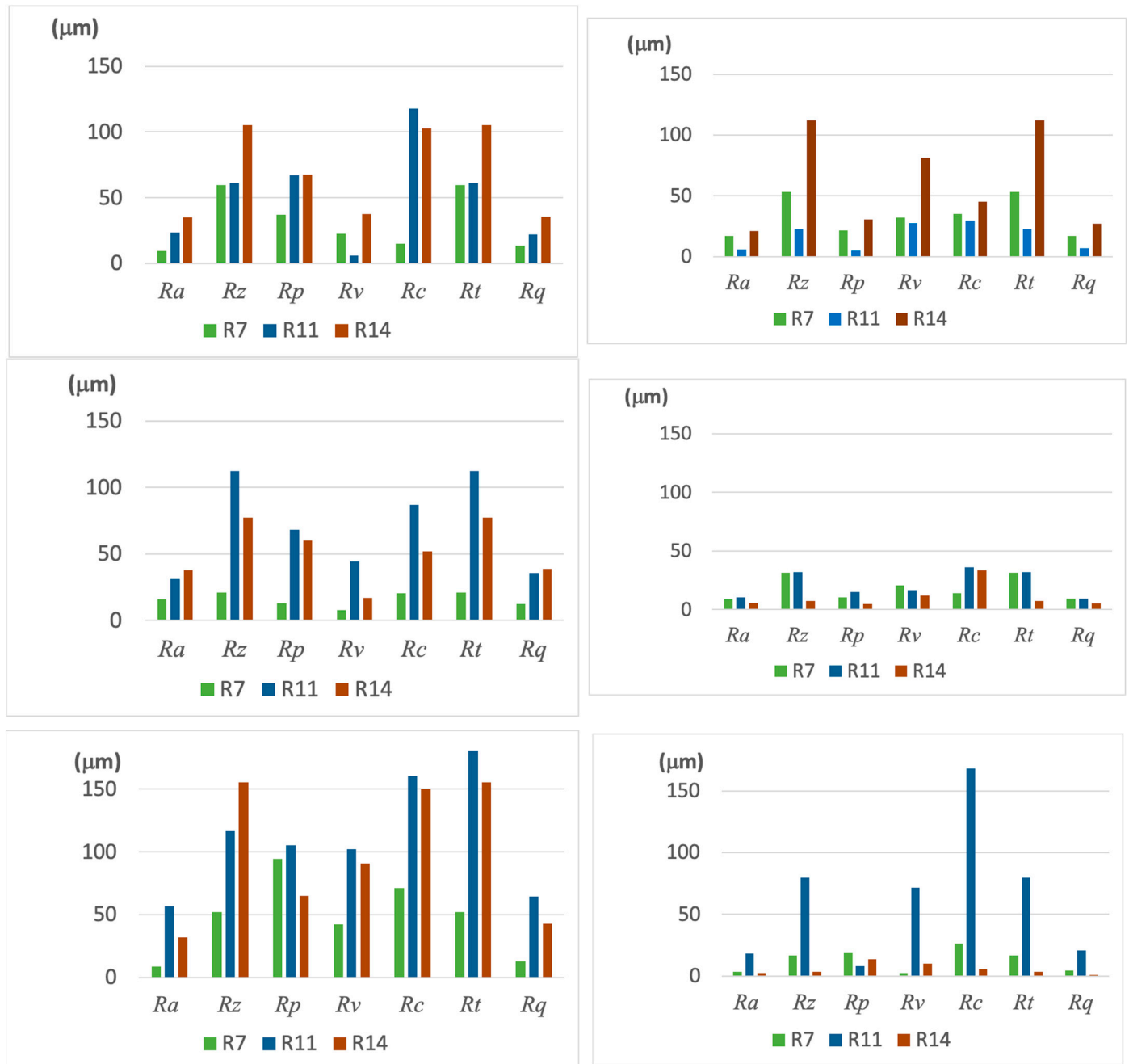


Figure 7. Roughness difference after and before wear test for Ti-Dia (left) and Ni-Dia (right) coatings for different measuring points: left (top), right (center) and top (bottom) measurements.

The difference in μm has been calculated considering the initial minus the final roughness when varying the sliding radius (7, 11, 14 mm) that is the linear speed. The plots report the roughness variation for the three measured points (left, top, right).

For each pin-on-disk test, the wear of the pin vs. disk in contact was calculated using the procedure described in [21].

The results of abrasion on the processed balls are reported in Figures 8 and 9. In Figure 8, the ball volume loss V_b (mm^3), the wear rate u ($\mu\text{m}/\text{h}$), and the wear coefficient k are calculated as described in [26] and then reported, while in Figure 9, the roughness

parameters measured on the abrasion surface of the balls are reported. It can be observed that, with increasing linear speed, the quality of abraded balls worsens when processed with Ni-Dia surfaces, while in the case of Ti-Dia surfaces, the effect of linear speed seems to improve the quality of the abraded surfaces.

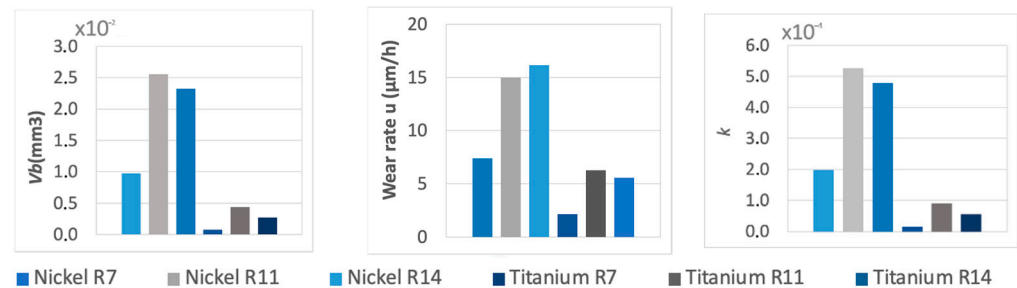


Figure 8. Wear parameters for Si₃N₄ balls.

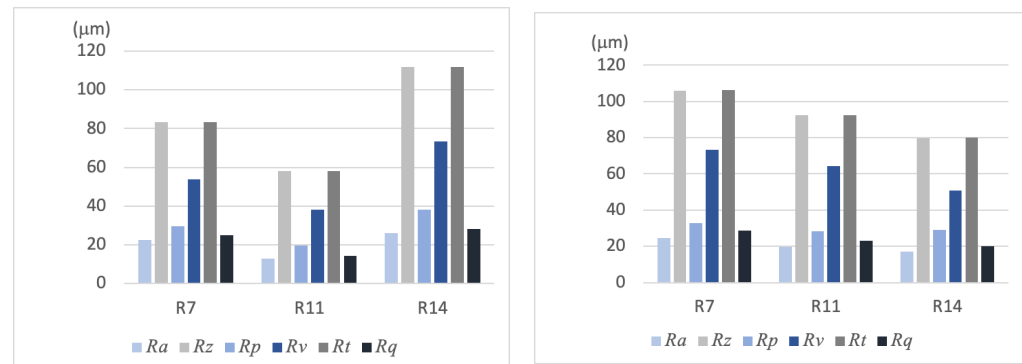


Figure 9. Surface roughness parameters for Si₃N₄ balls: worn by Ni-Dia (left) and Ti-Dia (right) coating.

The analysis of Figure 7 shows that along the wear race the inhomogeneities of the surface tend to be larger.

The roughness parameters show a different behavior both with the linear speed and with the measuring direction. For the Ti-Dia coating, the surface roughness parameters show an increment of all roughness parameters with increasing abrasion; furthermore, the lowest increment is obtained for the lowest linear speed, while for higher speed the behavior of the parameters seems to change with speed. If we consider the measurements obtained in the radial direction R_a and R_q increase with linear speed (R11 and R14), that is the arithmetic average and the root mean square roughness in the measuring length, two parameters related to average amplitude. R_z , R_p , R_c , and R_t either remain constant or decrease when changing from condition R11 to R14. R_p and R_v represent the maximum peak and the minimum valley measure, respectively, while R_z and R_t the maximum distance between maximum peak and minimum valley measured over the sampling length and the evaluation length, respectively. All these parameters are related to an increment of irregularities in the profile. It seems there is an intermediate linear speed between the maximum and minimum tested in the experiments, for which the abrasive coating is much more affected by the interaction with the ceramic pin. If we consider the measurements run parallel to linear speed the trend is the same for R_a , R_v , R_c , and R_t , that is for the lowest values for R9 then increasing for R11 and decreasing for R14 while R_z increases with linear speed.

In the Ni-Dia coating these increments are less evident and range one order of magnitude less than the Ti-Dia coating. It has to be noted that all the parameters related to R11 configuration measured in parallel direction can be compared to Ti-Dia values.

The Ti diamond coating is less resistant to abrasion, and the effect of the abrasion is to remove the highest peak.

The Ti-Dia coating shows the largest difference in roughness parameters, comparing before and after the pin-on-disk test. This means that the Ti-Dia coating at the end of the test shows a lower roughness than the Ni-Dia coating. Ti-Dia coatings tends to wear more than Ni diamond coatings. Unlike [26], the final roughness measurements were run after air cleaning of the disks, that is, after removal of powder debris. The final roughness can be attributed to displacing the metal coating from the diamond particles to the surrounding roughness valleys by means of a plastic deformation process. This phenomenon reduces the asperities of the abrasive coating and, therefore, its abrasion effectiveness, as shown in Figure 8 left, where the ball abraded volume V_b is reported. This deformation also affects the wear coefficient, as witnessed in Figure 8 right. This plastic behavior of cold sprayed pure Ni in tribological tests is also described in [13].

In [26], the test preload was lower (1 N vs. 5 N) and this wear effect on the disks was less evident. In [26], the average dimension of the particles was less than the half of the present ones. These differences can justify the large differences obtained both in the abraded volumes of the ball and the final roughness of the ball.

As for abrasive surfaces, the Ni-Dia abrasive coatings are more effective in terms of abraded volume on the balls, but the disk tends to wear faster; the opposite occurs for the Ti-Dia abrasive disk. The quality of abraded balls does not change strongly in the two cases (Figure 9). According to [26] the abraded volume on disks can be neglected.

4. Conclusions

The present research was developed with the aim of evaluating the applicability of the cold spray technique for obtaining performant abrasive coating to be used in ball ceramic processing. To this aim, the activity was focused on investigating how two commercial powders are deposited, and how they are modified by the deposition process and by the abrasion process.

Therefore, the present paper aimed at qualifying and quantifying the abrasion performance of abrasive diamond coatings obtained by means of cold spray technique with two commercial diamond-coated powders, with the aim of setting up the basis for an innovative manufacturing process for ceramic balls in hybrid bearings. The analysis was performed by means of inspecting the deposition process and pin-on-disk tests.

Coating adhesion, particle distribution, and the effect of the process on the roughness of the coating were analyzed. Pin-on-disk testing aimed at quantifying the quality of the abrasion measured as final roughness of the abraded balls, abraded volume, wear rate, and wear coefficient. To investigate the applicability of the process, the effect of abrasion on abrasive disks was further measured by means of roughness and profile measurements on the disks.

The pin-on-disk tests show a different abrasion performance for the different abrasive coatings and the different linear speed. The surface roughness variation is larger for Ti-Dia coatings than for the Ni-Dia coating, for all acquired roughness parameters. The abrasion rate increases with increasing speed when changing from R7 configuration to R11 configuration and then decreases slightly changing to R14 configuration, given the same testing length. The quality of the manufacturing process, in terms of roughness of the abraded balls, does not seem to be strongly affected by linear speed.

The Ti-Dia coating is more sensitive to abrasion than the Ni-Dia coating. Furthermore, the coatings are more damaged by higher local speed than by slower speed.

With increasing linear speed, the ball abraded volume increases and then slightly decreases for the same abrasion length; the same occurs for wear rate and wear coefficient, while for wear rate in the Ni-Dia coating it shows a maximum for R11 testing configuration, while for the Ti-Dia coating it increases with linear speed.

The Ti-Dia coating is more effective in abrasion than the Ni-Dia coating; furthermore, the Ni-Dia coating is less damaged and, therefore, it is more resistant to abrasion than the Ti-Dia coating.

Author Contributions: Conceptualization, I.P.F., R.S. and S.R.; methodology, R.L.; experimental testing, I.P.F. and P.Y.; resources, R.L. and S.R.; data curation, I.P.F. and R.S.; writing—original draft preparation, writing—review and editing, I.P.F. and R.S. All authors have read and agreed to the published version of the manuscript.

Funding: This research received no external funding.

Institutional Review Board Statement: Not applicable.

Informed Consent Statement: Not applicable.

Conflicts of Interest: The authors declare no conflict of interest.

References

1. Vieillard, C.; Brizmer, V.; Kadin, Y.; Morales-Espejel, G.E.; Gabelli, A. Benefits of Hybrid Bearings in Severe Conditions. *SKF Evol.* **2017**, *3*, 21–26.
2. Morales-Espejel, G.E.; Gabelli, A.; Félix-Quiñonez, A. The SKF Generalized Bearing Life Model (GBLM) for Hybrid Bearings. SKF Group 2021. PUB BU/P9 19277 EN. September 2019. Available online: <https://evolution.skf.com/the-skf-generalized-bearing-life-model-for-hybrid-bearings/> (accessed on 14 May 2022).
3. Gabelli, A.; Morales-Espejel, G.E. A model for hybrid bearing life with surface and subsurface survival. *Wear* **2019**, *422–423*, 223–234. [[CrossRef](#)]
4. Ghezzi, I.; Houara Komba, E.W.; Tonazzi, D.; Bouscharain, N.; Le Jeune, G.; Coudert, J.B.; Massi, F. Damage evolution and contact surfaces analysis of high-loaded oscillating hybrid bearings. *Wear* **2018**, *406–407*, 1–12. [[CrossRef](#)]
5. Yin, S.; Lupoi, R.; Chen, C. Property Enhancement of Cold Sprayed Al-Diamond MMC Coating by Using Core-Shelled Diamond Reinforcements. *Proc. Int. Therm. Spray Conf.* **2019**, *2019*, 469–475.
6. Lupoi, R.; Meyer, M.; Wits, W.W.; Yin, S. The Role of Particles Flow Characteristics in the Performance of Cold Spray Nozzles. *CIRP Ann.* **2020**, *69*, 189–192. [[CrossRef](#)]
7. Lux, B.; Haubner, R. Diamond Deposition on Cutting Tools. *Ceram. Int.* **1996**, *22*, 347–351. [[CrossRef](#)]
8. Morand, G.; Chevallier, P.; Bonilla-Gameros, L.; Turgeon, S.; Cloutier, M.; Da Silva Pires, M.; Sarkissian, A.; Tatoulian, M.; Houssiau, L.; Mantovani, D. On the Adhesion of Diamond-like Carbon Coatings Deposited by Low-pressure Plasma on 316L Stainless Steel. *Surf. Interface Anal.* **2021**, *53*, 658–671. [[CrossRef](#)]
9. Yin, S.; Xie, Y.; Cizek, J.; Ekoi, E.J.; Hussain, T.; Dowling, D.P.; Lupoi, R. Advanced Diamond-Reinforced Metal Matrix Composites via Cold Spray: Properties and Deposition Mechanism. *Compos. Part B Eng.* **2017**, *113*, 44–54. [[CrossRef](#)]
10. Silva, V.A.; Costa, F.M.; Fernandes, A.J.S.; Nazaré, M.H.; Silva, R.F. Influence of SiC particle addition on the nucleation density and adhesion strength of MPCVD diamond coatings on Si₃N₄ substrates. *Diam. Relat. Mater.* **2000**, *9*, 483–488. [[CrossRef](#)]
11. Haubner, R.; Kalss, W. Diamond deposition on hardmetal substrates—Comparison of substrate pre-treatments and industrial applications. *Int. J. Refract. Met. Hard Mater.* **2010**, *28*, 475–483. [[CrossRef](#)]
12. Zhang, C.; Ohmori, H.; Marinescu, I.; Kato, T. Grinding of Ceramic Coatings with Cast Iron Bond Diamond Wheels. A Comparative Study: ELID and Rotary Dresser. *Int. J. Adv. Manuf. Technol.* **2001**, *18*, 545–552. [[CrossRef](#)]
13. Padmini, B.V.; Mathapati, M.; Niranjana, H.B.; Sampathkumaran, P.; Seetharamu, S.; Ramesh, M.R.; Mohan, N. High temperature tribological studies of cold sprayed nickel based alloy on low carbon steels. *Mater. Today Proc.* **2020**, *27*, 1951–1958. [[CrossRef](#)]
14. Yin, S.; Cavaliere, P.; Aldwell, B.; Jenkins, R.; Liao, H.; Li, W.; Lupoi, R. Cold Spray Additive Manufacturing and Repair: Fundamentals and Applications. *Addit. Manuf.* **2018**, *21*, 628–650. [[CrossRef](#)]
15. Yin, S.; Cizek, J.; Yan, X.; Lupoi, R. Annealing Strategies for Enhancing Mechanical Properties of Additively Manufactured 316L Stainless Steel Deposited by Cold Spray. *Surf. Coat. Technol.* **2019**, *370*, 353–361. [[CrossRef](#)]
16. Xie, Y.; Yin, S.; Chen, C.; Planche, M.-P.; Liao, H.; Lupoi, R. New Insights into the Coating/Substrate Interfacial Bonding Mechanism in Cold Spray. *Scr. Mater.* **2016**, *125*, 1–4. [[CrossRef](#)]
17. Doubenskaia, M.; Latfulina, Y.S.; Samodurova, M.N. Cold Spray Deposition of Copper/Tungsten Composite Coatings. *IOP Conf. Ser. Mater. Sci. Eng.* **2020**, *969*, 012106. [[CrossRef](#)]
18. Fang, L.; Xu, Y.; Gao, L.; Suo, X.; Gong, J.; Li, H. Cold-Sprayed Aluminum-Silica Composite Coatings Enhance Anti-wear/Anticorrosion Performances of AZ31 Magnesium Alloy. *Adv. Mater. Sci. Eng.* **2018**, *2018*, 3215340. [[CrossRef](#)]
19. Yin, S.; Chen, C.; Suo, X.; Lupoi, R. Cold-Sprayed Metal Coatings with Nanostructure. *Adv. Mater. Sci. Eng.* **2018**, *2018*, 2804576. [[CrossRef](#)]
20. Aldwell, B.; Yin, S.; McDonnell, K.A.; Trimble, D.; Hussain, T.; Lupoi, R. A Novel Method for Metal–Diamond Composite Coating Deposition with Cold Spray and Formation Mechanism. *Scr. Mater.* **2016**, *115*, 10–13. [[CrossRef](#)]
21. ASTM-G99; Standard Test Method for Wear Testing with a Pin-on-Disk Apparatus. ASTM Standard: West Conshohocken, PA, USA, 1999.
22. ASTM G133; Standard Test Method for Linearly Reciprocating Ball-on-Flat Sliding Wear 1. ASTM Standard: West Conshohocken, PA, USA, 2011; pp. 1–10. [[CrossRef](#)]
23. Jana, A.; Dandapat, N.; Das, M.; Balla, V.K.; Chakraborty, S.; Saha, R.; Mallik, A.K. Severe Wear Behaviour of Alumina Balls Sliding against Diamond Ceramic Coatings. *Bull. Mater. Sci.* **2016**, *39*, 573–586. [[CrossRef](#)]

24. Qin, W.; Yue, W.; Wang, C. Controllable Wear Behaviors of Silicon Nitride Sliding against Sintered Polycrystalline Diamond via Altering Humidity. *J. Am. Ceram. Soc.* **2018**, *101*, 2506–2515. [[CrossRef](#)]
25. Li, Y.; Sha, X.; Yue, W.; Qin, W.; Wang, C. Effects of Tribochemical Reaction on Tribological Behaviors of Si₃N₄/Polycrystalline Diamond in Hydrochloric Acid. *Int. J. Refract. Met. Hard Mater.* **2019**, *79*, 197–203. [[CrossRef](#)]
26. Pessolano Filos, I.; Sesana, R.; Di Biase, M.; Lupoi, R. New Abrasive Coatings: Abraded Volume Measurements in Ceramic Ball Production. *J. Manuf. Mater. Process.* **2021**, *5*, 81. [[CrossRef](#)]